Ionic Liquid Electrolytes

For decades, improvements in electrolytes and electrodes have driven the development of electrochemical energy storage devices. Generally, electrodes and electrolytes should not be developed separately due to the importance of the interaction at their interface. The energy storage ability and safety of energy storage devices are in fact determined by the arrangement of ions and electrons between the electrode and the electrolyte.

▌ 1. Introduction

Energy storage system (ESS) and electric vehicle (EV) markets have been growing every year, and various types of energy storage devices are struggling to enter the market [1][2]. In particular, fuel cells (FCs), lithium-ion batteries (LIBs), and supercapacitors (SCs) are competing with one another in the EV market [3]. FCs have attracted a great deal of attention as energy conversion devices [4]. However, there remain difficulties in their commercialization based on the disadvantages associated with transporting, storing H_2, and the reluctance to establish H_2 stations [5][6][7]. Further, because of their narrow operating voltage (theoretically 1.23 V), a stacking process is essential for the application of FCs [8]. In addition, the reaction to convert hydrogen and oxygen into water is highly exothermic, thus FCs face heat management issues [9][10][11][12][13].

To overcome conventional electrolyte issues, many researchers have been focused on ionic liquids (ILs). At the early stage, ILs were studied as solvents. Generally, organic solvents used as reaction solvents in various chemical processes are highly volatile and explosive, and most of them are harmful to the human body [14]. Therefore, for developing environmentally friendly processes, many researchers are working on the development of next-generation solvents that can replace organic solvents.

Because of the advantages of the ILs, their market is steadily growing. The global IL market was estimated to be US $20 million by 2015, of which the solvent and catalyst market was the largest with US $6 million, and the market for ILs is expected to grow due to the expansion of the application field, particularly in the growth of the energy storage field. The application fields of ILs can be divided into solvents and catalysts, energy storage, separation and extraction, and biorefinery, and among these the energy storage field with high growth potential was examined [15].

Also, acronyms and properties of representative ILs are provided in **Table 1** and **Table 2** along with descriptions of ILs used in various fields of energy storage.

Table 1. The lists of the representative ILs applied in LIBs and SCs as electrolytes.

Classification	Acronyms	Ionic Liquid	Reference(s)
Li-ion batteries	[PMI][TFSI]	1-propyl-3-methylimidazolium bis(trifluoromethylsulfonyl)imide	[70]
	[BMI][TFSI]	1-Butyl-3-methylimidazolium bis(trifluoromethylsulfonyl)imide	[70]
	[EMI][TFSI]	1-ethyl-2,3trimethyleneimidazolium bis(trifluoromethane sulfonyl)imide	[72]
	[PP$_{13}$][TFSI]	N-methyl-N-propylpiperidinium Bis(trifluoromethanesulfonyl)imide	[73]
	[Pyr$_{14}$][DCA]	N-butyl-N-methyl pyrrolidinium-dicyanamide	[74]
	[Pyr$_{14}$][TFSI]	N-butyl-N-methyl pyrrolidinium bis(trifluoromethylsulfonyl)imide	[74]
	[Pyr$_{14}$][TFSAM]	N-butyl-N-methyl pyrrolidinium bis(trifluoromethylsulfonyl)-N-cyanoamide	[74]
	[N$_2$(2o1)$_3$][TFSI]	N-ethyl-N,N,N-tri-(2-methoxyethyl)ammonium bis(trifluoromethanesulfonyl)imide	[75]
	[(N$_2$(2o1)$_2$(2o2)][TFSI]	N-ethyl-N,N-di-(2-methoxyethyl)-N-2-ethoxyethylammonium bis(trifluoromethanesulfonyl)imide	[75]
	[(N$_3$(2o1)$_3$)][TFSI]	N-propyl-N,N,N-tri-(2-methoxyethyl)ammonium bis(trifluoromethanesulfonyl)imide	[75]
	[(N$_4$(2o1)$_3$)][TFSI]	N-butyl-N,N,N-tri-(2-methoxyethyl)ammonium bis(trifluoromethanesulfonyl)imide	[75]
	[C$_4$mpyr][TFSI]	N-methyl-N-butyl-pyrrolidinium bis(trifluoromethanesulfonyl)imide	[76]
	[PfM$_{pyr}$][FSI]	1-Methyl-1-propyl-3-fluoropyrrolidinium bis(fluorosulfonyl)-imide	[77]
	[C$_3$mpyr][FSI]	N-methyl-N-propyl-pyrrolidinium (fluorosulfonyl) imide	[78]
LiS batteries	[PP$_{13}$][TFSI]	N-methyl-N-propylpiperidinium bis(trifluoromethanesulfonyl)imide	[79]
	[LiG$_3$][TFSI]	Li(triglyme) bis(trifluoromethylsulfonyl)imide	[80]
	PEO, LiTFSI-[TBP][HP]	poly(ethyleneoxide)-lithium bis(trifluoromethylsulfonyl)imide-tetrabutylphosphonium 2-hydroxypyridine	[81]
	PVdF-HFP/PMMA/[BMI][BF$_4$]	(poly(vinylidene fluoride-co-hexafluoropropylene)/poly(methyl methacrylate)- 1-butyl-3-methylimidazolium tetrafluoroborate))	[82]
	PVdF-HFP/[EMI][DCA]	(poly(vinylidene fluoride-co-hexafluoropropylene)/1-ethyl-3-methylimidazolium dicyanamide))	[83]
	PVdF-HFP/[EMI][TFSI]/rGO-PEG-NH$_2$	(poly(vinylidene fluoride-co-hexafluoropropylene)/ (covalent linked 2,2″-(ethylenedioxy) bis (ethylamine) to reduced graphene oxide))	[84]

Classification	Acronyms	Ionic Liquid	Reference(s)
Supercapacitors	[EMI][BF$_4$]	1-ethyl-3-methylimidazolium tetrafluoroborate	[85]
	[EMI][FSI]	1-ethyl-3-methyleneimidazolium (fluorosulfonyl) imide	[86]
	[Pyr$_{14}$][TFSI]	N-butyl-N-methyl pyrrolidinium bis(trifluoromethylsulfonyl)imide	[87]
	[EMI][TFSI]	1-ethyl-3-methyleneimidazolium bis(trifluoromethane sulfonyl)imide	[88]
	[Pyr$_{14}$][FSI]	N-ethyl-N-methylpyrrolidinium (fluorosulfonyl) imide	[89]
	[PIP$_{13}$][FSI]	N-methyl-N-propylpiperidinium (fluorosulfonyl)imide	[89]
	[Pyr][TFSI]	N-butyl-N-methyl pyrrolidinium bis(trifluoromethylsulfonyl)imide	[90]
	[PMP$_{yrr}$][TFSI]	1-Methyl-1propylpyrrolidinium bis(trifluoromeyhanesulfonyl)imide	[91]
	[BTM][TFSI]	Butyltrimethylammonium- bis(trifluoromethylsulfonyl)imide	[92]
	[TEA][TFSI]	Trimethylamine- bis(trifluoromethylsulfonyl)imide	[93]
Quasi-solid-state supercapacitors	PHEMA-co-PEGDMA/[EMI][BF$_4$]	poly(2-hydroxyethyl methacrylate) and poly(ethylene glycol) diacrylate/1-ethyl-3-methylimidazolium tetrafluoroborate	[94]
	[BMI][I]	1-butyl-3-methylimidazolium iodide	[95]
	[BMI][Cl]	1-butyl-3-methylimidazolium chloride	[96]
	PVdF-HFP/[EMI][BF$_4$]	(poly(vinylidene fluoride-co-hexafluoropropylene) /- 1-ethyl-2,3methylimidazolium tetrafluoroborate))	[97]
	PUA/[EMI][TFSI]	(polyurethane acrylate-(1-ethyl-3-methylimidazolium-bis(trifluoromethylsulfonyl)imide)	[98]
All-solid-state supercapacitors	[Pyr$_{14}$][TFSI]	1-butyl-1-methylpyrrolidinium bis (trifluoromethanesulfonyl)) imide	[99]
	[Pyr$_{14}$][DCA]	1-butyl-1-methylpyrrolidinium dish Amide	[99]
	[PIL][TFSI]	poly(diallyldi-methylammonium) bis (trifluoromethylsulfonyl) imide	[100]
	[EMI][FSI]	1-ethyl-3-methyleneimidazolium (fluorosulfonyl) imide	[100]
	[MBI][FSI]	1-methyl-3-butylimidazolium (fluorosulfonyl) imide	[100]
	[DPI][TFSI]	1,2-dimethyl-3-propylimidazolium bis(tri-fluoromethylsulfonyl) imide	[100]

Table 2. The properties of representative ILs.

Type of Cation	Ionic Liquid	Melting Point (°C)	Density (g mL^{-1}) at 25 °C (lit.)	Cnductivity (mS cm^{-1})	Electrochemical Stability Window (V)	Reference(s)
Imidazolium	[EMI][BF$_4$]	15	1.294	13–15	4 (ref. elecrode: carbon)	[101,102]
	[EMI][TFSI]	−15	1.53	8–10	3.5–3.7 (ref. elecrode: carbon)	[91]
	[BMI][TFSI]	1	1.44	3.9	4.5–5 (ref. elecrode: carbon)	[70]
Pyrrolidinum	[Pyr$_{14}$][TFSI]	−6	1.4216	2.5–3	3.5 (ref. elecrode: carbon)	[103]
	[Pyr$_{14}$][DCA]	−55	0.95	10.8	3 (ref. elecrode: carbon)	[104]

Type of Cation	Ionic Liquid	Melting Point (°C)	Density (g mL^{-1}) at 25 °C (lit.)	Cnductivity (mS cm^{-1})	Electrochemical Stability Window (V)	Reference(s)
Piperidinium	[PP$_{13}$][TFSI]	12	151	1.4	5–6 (ref. electrode: Li)	[73]
	[PP$_{13}$][FSI]		95	3.7	5–6 (ref. electrode: Li)	[73]

2. Ionic Liquids for Lithium-Ion Battery Electrolytes

In 2010, Zaghib proposed [EMI][TFSI] as an additive to the electrolyte for LIBs, demonstrating an increase in the thermal stability of the electrolyte [16]. Chen et al. reported that bis(fluorosulfonyl)imide lithium salt ([LiTFSI]) and the [PP 13][TFSI] electrolyte significantly improve rate capacity and low temperature performance and are safer than conventional electrolytes [17]. In addition, inorganic alkali salts with relatively low melting points were used to improve the cycle stability and high performance of LIBs, even at high temperatures. For instance, Zhibin et al. found that dual-salt-mixed potassium bis(fluorosulfonyl)imide ([KFSI]) and [LiFSI] exhibited high ionic conductivity (10 −3 ~10 −2 S cm −1) from 40–150 °C [18]. In addition, designs for ionic structures and the addition of an additive to affect the properties of ILs were reported, as ILs are tunable with regard to polarity and basicity of acidity. For instance, [EMI][TFSI], [PMI][TFSI], and [BMI][TFSI] were selected as electrolytes and their electrochemical properties were investigated [19]. It was found that [EMI][TFSI] exhibited the best electrochemical performance and thermal stability. In 2009, Karna et al. synthesized several quaternary ammonium ILs based on cations with two identical ether groups and have studied quaternary ammonium-based ILs [20]. Yang et al. reported five low viscosity quaternary ammonium-based ILs [N 2(2o1) 3][TFSI], [(N 3(2o1) 3)][TFSI], [(N 4(2o1) 3)][TFSI]; these ILs were applied to LIBs. Among these IL electrolytes, [(N 2(2o1) 2(2o2)][TFSI] and [N 2(2o1) 3][TFSI] showed the best capacity and cycle characteristics at 0.1 C [21]. In 2014, Hirano et al. synthesized an organosilicon functionalized ammonium IL with an oligo (ethylene oxide) substituent. All ILs synthesized in this way contained large cations and had low viscosity (125–173 cP) at room temperature (RT) and showed superior thermal stability with higher decomposition temperatures (310–350 °C) and a 3.9 V–4.7 V stability window. However, they were not suitable for LIB electrolytes due to their low conductivity. Therefore, organosilicon functionalized ammonium ILs with an oligo (ethylene oxide) substituent were mixed with a commercial carbonate electrolyte to form a hybrid electrolyte. At a doping content of 30 vol%, the lithium iron phosphate (LFP) electrode/Li half-cell showed excellent reversible capacity, cycle stability, and effectively suppressed electrolyte degradation due to stable SEI formation, thus improving lithium storage performance [22]. In 2019, Hahime et al. reported that by replacing the conventional carbonate electrolyte with an RT quaternary ammonium-based electrolyte, [C 4mpyr][TFSI], decomposition of organic solvents was suppressed and short-circuiting caused by Li dendrite formation was prevented. In the above study, the authors investigated the morphology of Li electrodeposition obtained from the [C 4mpyr][TFSI] electrolyte and clarified the correlation between electrochemical parameters and Li deposition morphology. The surface resistance was temperature-dependent and also affected deposition polarizations and nucleation. As a result, to suppress the Li dendrite growth during cycling, the deposition polarization should be expanded during deposition while simultaneously increasing the Li diffusion coefficient of the electrolyte [23].

Recently, [Pyr 14], [Pyr 13], and [Pyr 15] were broadly studied for LIBs due to their high ionic conductivity and superior electrochemical performance [24][25][26]. The electrochemical performance of the LiNi 0.5 Co 0.2 Mn 0.3 O 2 (NCM 523)/graphite full cells was also studied by Paillard et al. These studies found that [Pyr 14][TFSI], [Pyr 14][DCA], and [Pyr 14][TFSAM] exhibited higher electrochemical performances than organic carbonate solvent-based electrolytes in NCM 523 and graphite full cells [27]. As the demand for energy storage devices increases, ILs with high stability, good cycle characteristics, and resistance to continuously changing temperatures have emerged. Since 2020, a method based on increasing salt concentration has been used with ILs. Qian et al. achieved high oxidation stability (>5.5 V vs. Li + /Li) for a graphite and Li metal anode by increasing the LiTFSI salt concentration to 4 M with [PfM pyr][FSI], leading to superior electrochemical cycling stability [24]. Howlett et al. reported an LIB with a high energy density system that suppressed dendritic growth despite the fast charging rate by using LiFSI salt and [C 3mpyr][FSI]. Operating at high current densities increased coulombic efficiency up to 96% at 20 mA cm −2 with a 0.2 V polarization. A more detailed morphological study showed that sediment evolution remained dendrite-free and uniform with low electrode resistance (**Figure 1**). X-ray photoelectron microscopy (XPS), time-of-flight secondary ion mass spectrometry (ToF-SIMS), and scanning electron microscopy (SEM) surface measurements revealed that a LiF-rich SEI layer with a lack of organic components was formed. Reduced dendrite formations at high current densities are further emphasized by a 500 cycle at 10 mA cm −2 using a porous separator in coin cell cycling [28]. Although the conductivity of these IL-based electrolytes is lower than that of conventional carbonate electrolytes (8–12 mS cm −1) , the overall performance of the full cell does not decrease much and is rather superior in terms of stability of the battery.
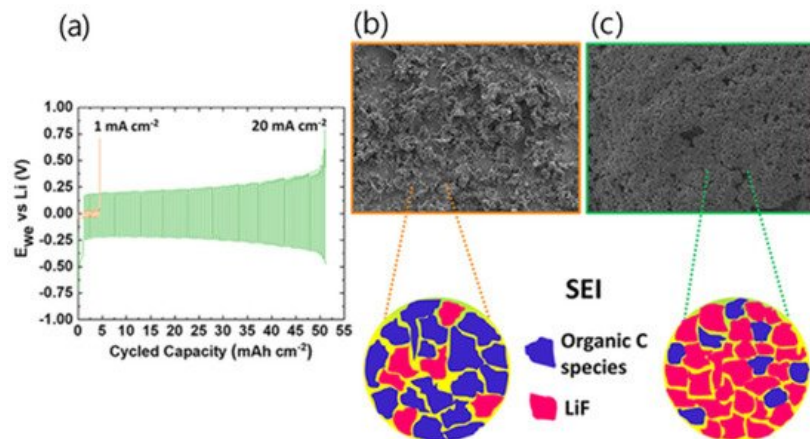
Figure 1. (**a**) Symmetric voltage profile at different current densities; (**b**) SEM images of deposited lithium at 1 mA cm^{-2}; (**c**) SEM image of deposited lithium at 20 mA cm^{-2}. Reprinted 2020 from [78] with permission from American Chemical Society.

In 1979, after demonstrating the solubility of poly(ethylene oxide) (PEO) against lithium salts, solid polymer electrolytes (SPEs) became widely used in LIBs [29][30][31][32]. Many researchers have since added ILs and lithium salts to escalate the ionic conductivity of PEO.

In 2017, Rhee et al. reported an IL-doped PEO-based solid electrolyte, studying the conductivity and cycle stability of the Li/SPE/LFP. The electrolyte was composed of PEO, lithium difluoro(oxalato)borate (LIFOB), and [EMI][TFSI] [31]. When 40 wt% of ILs was added at room temperature, the SPE exhibited an ionic conductivity of 0.185 × 10 −3 S cm −1 , with improved electrochemical stability and a first discharge capacity of 155 mA h g −1 , which remained at 134.2 mA h g −1 after 50 cycles. In 2019, Wu et al. reported a flexible IL-based hybrid SPE electrolyte [29]. The hybrid SPE was fabricated with PEO, LiTFSI- [TBP][HP]. The SPE exhibited an ionic conductivity of 9.4 × 10 −4 S cm −1 , a wide electrochemical window over 5.0 V. The ionic conductivity of the PI solid electrolyte was 2.3 × 10 −4 S cm −1 at 30 °C.

3. Ionic Liquids for Supercapacitor Electrolytes

Xie et al. proposed an SC based on redox-active ILs by modifying the cations or anions with ferrocene to minimize self-discharge [33]. The modified IL-based SC exhibited an operating voltage of 2.5 V and an energy density of 13.2 Wh kg −1 , which was 83% higher than that of the unmodified IL-based SCs.

The electrochemical performance of SCs applied with [TEA][TFSI] mediated with hydroquinone (HQ) was studied and AC was adopted as an electrode for these SCs [34]. The specific capacitance was increased from 42 F g −1 to 72 F g −1 at 0.57 mA cm −2 when 0.3 M HQ was added to [TEA][TFSI]. The pseudo-capacitance contribution of HQ with the faradaic reaction of HQ/Q led to these results (**Figure 2**).
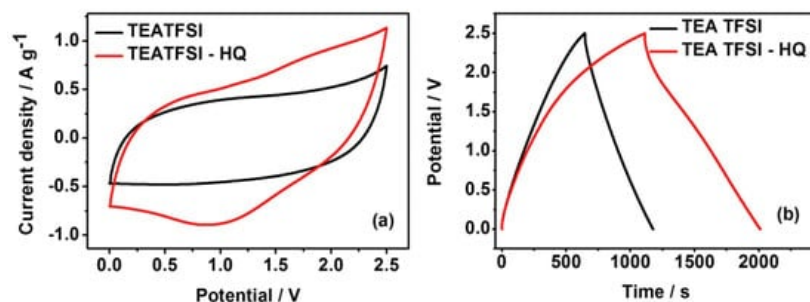

Figure 2. (**a**) Cyclic voltammograms of the SC at 10.0 mV s^{-1}; (**b**) galvanostatic charge–discharge at 0.57 mA cm^{-2} in neat [TEA][TFSI] and [TEA][TFSI]/HQ (0.3 M). Reprinted 2015 from [143] with permission from Elsevier.

The prototype ion gel electrolytes consist of ILs, organic solvents, and polymers, so-called gel polymer electrolytes of energy storage devices. In 1997, Fuller et al. reported an ion gel using PVdF-HFP as the polymer matrix [35][36]. The ion gel consisting of [EMI][BF 4], [EMI][CF 3SO 3], and PVdF-HFP achieved an ionic conductivity of 5.8 mS cm −1 . Ghamouss et al. presented a quasi-solid electrolyte that was combined methacrylate and dimethacrylate oligomers dissolved in [PMPyrr][TFSI] via free radical polarization, as shown in **Figure 3** . The advantage of this incorporation is that

the formed electrolyte can be used as a separator, is leakage-free, and provides a wide electrochemical stability window. The SC that used the prepared electrolyte showed a specific energy density of 16 Wh Kg $^{-1}$, a power density of 1.1 kW kg $^{-1}$, and coulombic efficiency of 99.9%.
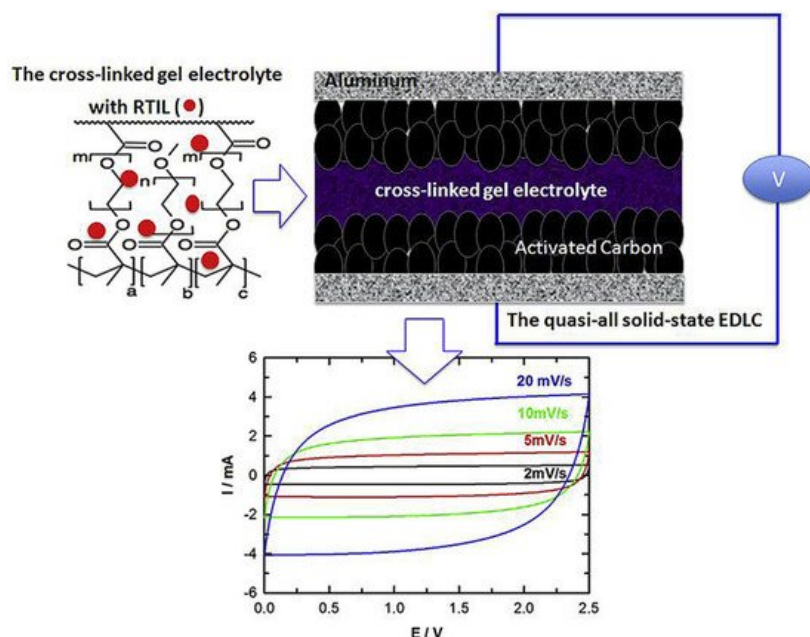

Figure 3. The scheme of the cross-linked gel polymer electrolyte that is composite with methacrylate and dimethacrylate oligomers dissolved in [PMPyrr][TFSI] followed by a cyclic voltammogram depending on scan rates. Reprinted 2011 from [64] with permission from Elsevier.

Furthermore, Yadav et al. used a dual redox-additive material (KI and diphenylamine (DPA)) to maximize the redox reaction at the electrode/electrolyte interface in non-aqueous gel polymer electrolytes with [BMI][TFSI] [37]. The proposed electrolytes showed a wide potential window (6.2 V vs. Ag), high ionic conductivity (σ = ~0.452 × 10 $^{-2}$ S cm $^{-1}$), high flexibility, free-standing properties, and remarkable thermal stability at up to 230 °C. Furthermore, the synergistic effect of the dual redox-additive material results in high specific energy and power densities of about 73.2 Wh kg $^{-1}$ and 34.8 kW kg $^{-1}$, respectively, with an enhanced specific capacitance of 337 F g $^{-1}$.

4. Conclusions and Prospective

With the continuous development of energy storage and conversion systems, ILs have played an important role in energy storage and conversion systems to enhance the electrochemical characteristics, reliability, and safety of these systems.

ILs have been used as an electrolyte for LIBs in various methods: (i) organic solvents have been replaced with ILs to reduce volatility and flammability, (ii) ILs have been mixed with conventional organic electrolytes to suppress electrolyte degradation due to stable SEI layer formation, thereby improving lithium storage performance, (iii) ILs have been used to minimize polysulfide dissolution, and (iv) ILs have been used with PEO and PVdF-HFP to improve the low conductivity of solid electrolytes.

References

1. Wang, L.; Guo, M.; Zhan, J.; Jiao, X.; Chen, D.; Wang, T. A new design of an electrochromic energy storage device with high capacity, long cycle lifetime and multicolor display. J. Mater. Chem. A 2020, 8, 17098–17105.

2. Pomerantseva, E.; Bonaccorso, F.; Feng, X.; Cui, Y.; Gogotsi, Y. Energy storage: The future enabled by nanomaterials. Science 2019, 366.

3. Macías, A.; Kandidayeni, M.; Boulon, L.; Trovão, J. Passive and Active Coupling Comparison of Fuel Cell and Supercapacitor for a Three-Wheel Electric Vehicle. Fuel Cells 2020, 20, 351–361.

4. Jacobson, M.Z.; Colella, W.G.; Golden, D.M. Atmospheric science: Cleaning the air and improving health with hydrogen fuel-cell vehicles. Science 2005, 308, 1901–1905.

5. Barthelemy, H.; Weber, M.; Barbier, F. Hydrogen storage: Recent improvements and industrial perspectives. Int. J. Hydrogen Energy 2017, 42, 7254–7262.

6. Moradi, R.; Groth, K.M. Hydrogen storage and delivery: Review of the state of the art technologies and risk and reliability analysis. Int. J. Hydrogen Energy 2019, 44, 12254–12269.

7. Tarkowski, R. Underground hydrogen storage: Characteristics and prospects. Renew. Sustain. Energy Rev. 2019, 105, 86–94.

8. Wang, J.; Wang, H.; Fan, Y. Techno-Economic Challenges of Fuel Cell Commercialization. Engineering 2018, 4, 352–360.

9. Lee, Y.D.; Ahn, K.Y.; Morosuk, T.; Tsatsaronis, G. Environmental impact assessment of a solid-oxide fuel-cell-based combined-heat-and-power-generation system. Energy 2015, 79, 455–466.

10. Elmer, T.; Worall, M.; Wu, S.; Riffat, S.B. Fuel cell technology for domestic built environment applications: State of-the-art review. Renew. Sustain. Energy Rev. 2015, 42, 913–931.

11. Buonomano, A.; Calise, F.; d'Accadia, M.D.; Palombo, A.; Vicidomini, M. Hybrid solid oxide fuel cells-gas turbine systems for combined heat and power: A review. Appl. Energy 2015, 156, 32–85.

12. Arsalis, A. A comprehensive review of fuel cell-based micro-combined-heat-and-power systems. Renew. Sustain. Energy Rev. 2019, 105, 391–414.

13. Ellamla, H.R.; Staffell, I.; Bujlo, P.; Pollet, B.G.; Pasupathi, S. Current status of fuel cell based combined heat and power systems for residential sector. J. Power Sources 2015, 293, 312–328.

14. Flamme, B.; Rodriguez Garcia, G.; Weil, M.; Haddad, M.; Phansavath, P.; Ratovelomanana-Vidal, V.; Chagnes, A. Guidelines to design organic electrolytes for lithium-ion batteries: Environmental impact, physicochemical and electrochemical properties. Green Chem. 2017, 19, 1828–1849.

15. Kunal, A.; Mamtani, K. Ionic Liquids Market Size, Share & Trends Analysis Report by Application (Solvents & Catalysts, Extractions & Separations, Bio-Refineries, Energy Storage), By Region, And Segment Forecasts, 2018–2025; Report ID GVR-1-68038-283-9; Global Market Insights: Lexington, MA, USA, 2015.

16. Guerfi, A.; Dontigny, M.; Charest, P.; Petitclerc, M.; Lagacé, M.; Vijh, A.; Zaghib, K. Improved electrolytes for Li-ion batteries: Mixtures of ionic liquid and organic electrolyte with enhanced safety and electrochemical performance. J. Power Sources 2010, 195, 845–852.

17. Xiang, H.F.; Yin, B.; Wang, H.; Lin, H.W.; Ge, X.W.; Xie, S.; Chen, C.H. Improving electrochemical properties of room temperature ionic liquid (RTIL) based electrolyte for Li-ion batteries. Electrochim. Acta 2010, 55, 5204–5209.

18. Mai, Y.J.; Luo, H.; Zhao, X.Y.; Wang, J.L.; Davis, J.; Lyons, L.J.; Zhang, L.Z. Organosilicon functionalized quaternary ammonium ionic liquids as electrolytes for lithium-ion batteries. Ionics 2014, 20, 1207–1215.

19. Barbosa, J.C.; Correia, D.M.; Gonçalves, R.; de Zea Bermudez, V.; Silva, M.M.; Lanceros-Mendez, S.; Costa, C.M. Enhanced ionic conductivity in poly(vinylidene fluoride) electrospun separator membranes blended with different ionic liquids for lithium ion batteries. J. Colloid Interface Sci. 2021, 582, 376–386.

20. Yang, B.; Li, C.; Zhou, J.; Liu, J.; Zhang, Q. Pyrrolidinium-based ionic liquid electrolyte with organic additive and LiTFSI for high-safety lithium-ion batteries. Electrochim. Acta 2014, 148, 39–45.

21. Fang, S.; Jin, Y.; Yang, L.; Hirano, S.I.; Tachibana, K.; Katayama, S. Functionalized ionic liquids based on quaternary ammonium cations with three or four ether groups as new electrolytes for lithium battery. Electrochim. Acta 2011, 56, 4663–4671.

22. Beltrop, K.; Qi, X.; Hering, T.; Röser, S.; Winter, M.; Placke, T. Enabling bis(fluorosulfonyl)imide-based ionic liquid electrolytes for application in dual-ion batteries. J. Power Sources 2018, 373, 193–202.

23. Sano, H.; Kitta, M.; Shikano, M.; Matsumoto, H. Effect of Temperature on Li Electrodeposition Behavior in Room-Temperature Ionic Liquids Comprising Quaternary Ammonium Cation. J. Electrochem. Soc. 2019, 166, A2973–A2979.

24. Liu, Q.; Hsu, C.W.; Dzwiniel, T.L.; Pupek, K.Z.; Zhang, Z. A fluorine-substituted pyrrolidinium-based ionic liquid for high-voltage Li-ion batteries. Chem. Commun. 2020, 56, 7317–7320.

25. Xu, F.; Liu, C.; Feng, W.; Nie, J.; Li, H.; Huang, X.; Zhou, Z. Molten salt of lithium bis(fluorosulfonyl)imide (LiFSI)-potassium bis(fluorosulfonyl)imide (KFSI) as electrolyte for the natural graphite/LiFePO4 lithium-ion cell. Electrochim. Acta 2014, 135, 217–223.

26. Kärnä, M.; Lahtinen, M.; Valkonen, J. Preparation and characterization of new low melting ammonium-based ionic liquids with ether functionality. J. Mol. Struct. 2009, 922, 64–76.

27. Hoffknecht, J.P.; Drews, M.; He, X.; Paillard, E. Investigation of the N-butyl-N-methyl pyrrolidinium trifluoromethanesulfonyl-N-cyanoamide (PYR14TFSAM) ionic liquid as electrolyte for Li-ion battery. Electrochim. Acta 2017, 250, 25–34.

28. Periyapperuma, K.; Arca, E.; Harvey, S.; Pathirana, T.; Ban, C.; Burrell, A.; Pozo-Gonzalo, C.; Howlett, P.C. High Current Cycling in a Superconcentrated Ionic Liquid Electrolyte to Promote Uniform Li Morphology and a Uniform LiF-Rich Solid Electrolyte Interphase. ACS Appl. Mater. Interfaces 2020, 12, 42236–42247.

29. Xie, Z.; Wu, Z.; An, X.; Yoshida, A.; Wang, Z.; Hao, X.; Abudula, A.; Guan, G. Bifunctional ionic liquid and conducting ceramic co-assisted solid polymer electrolyte membrane for quasi-solid-state lithium metal batteries. J. Memb. Sci. 2019, 586, 122–129.

30. Schaefer, J.L.; Lu, Y.; Moganty, S.S.; Agarwal, P.; Jayaprakash, N.; Archer, L.A. Electrolytes for high-energy lithium batteries. Appl. Nanosci. 2012, 2, 91–109.

31. Polu, A.R.; Rhee, H.W. Ionic liquid doped PEO-based solid polymer electrolytes for lithium-ion polymer batteries. Int. J. Hydrogen Energy 2017, 42, 7212–7219.

32. Zhu, L.; Zhu, P.; Fang, Q.; Jing, M.; Shen, X.; Yang, L. A novel solid PEO/LLTO-nanowires polymer composite electrolyte for solid-state lithium-ion battery. Electrochim. Acta 2018, 292, 718–726.

33. Gogotsi, Y.; Nikitin, A.; Ye, H.; Zhou, W.; Fischer, J.E.; Yi, B.; Foley, H.C.; Barsoum, M.W. Nanoporous carbide-derived carbon with tunable pore size. Nat. Mater. 2003, 2, 591–594.

34. Xie, H.J.; Gélinas, B.; Rochefort, D. Redox-active electrolyte supercapacitors using electroactive ionic liquids. Electrochem. Commun. 2016, 66, 42–45.

35. Pandey, G.P.; Liu, T.; Hancock, C.; Li, Y.; Sun, X.S.; Li, J. Thermostable gel polymer electrolyte based on succinonitrile and ionic liquid for high-performance solid-state supercapacitors. J. Power Sources 2016, 328, 510–519.

36. Austen Angell, C.; Ansari, Y.; Zhao, Z. Ionic Liquids: Past, present and future. Faraday Discuss. 2012, 154, 9–27.

37. Yadav, N.; Hashmi, S.A. Energy enhancement of quasi-solid-state supercapacitors based on a non-aqueous gel polymer electrolyteviaa synergistic effect of dual redox additives diphenylamine and potassium iodide. J. Mater. Chem. A 2020, 8, 18266–18279.